

Article

Estimation of Aboveground Biomass Using Manual Stereo Viewing of Digital Aerial Photographs in Tropical Seasonal Forest

Katsuto Shimizu ^{1,*}, Tetsuji Ota ¹, Tsuyoshi Kajisa ², Nobuya Mizoue ¹, Shigejiro Yoshida ¹, Gen Takao ³, Yasumasa Hirata ³, Naoyuki Furuya ⁴, Takio Sano ⁵, Sokh Heng ⁶ and Ma Vuthy ⁶

¹ Faculty of Agriculture, Kyushu University, 6-10-1 Hakozaki, Fukuoka 812-8581, Japan; E-Mails: chochoji1983@gmail.com (T.O.); mizoue@agr.kyushu-u.ac.jp (N.M.); syoshida@agr.kyushu-u.ac.jp (S.Y.)

² Faculty of Agriculture, Kagoshima University, 1-21-24 Korimoto, Kagoshima 890-8580, Japan; E-Mail: k2083442@agri.kagoshima-u.ac.jp

³ Department of Forest Management, Forestry and Forest Products Research Institute, 1 Matsunosato, Tsukuba 305-8687, Japan; E-Mails: takaogen@affrc.go.jp (G.T.); hirat09@affrc.go.jp (Y.H.)

⁴ Hokkaido Research Center, Forestry and Forest Products Research Institute, 7 Hitsujigaoka, Toyohiraku, Sapporo 062-8516, Japan; E-Mail: nfuruya@affrc.go.jp

⁵ Asia Air Survey Company, LTD, Shinyuri 21 Building, 1-2-2 Manpukuji, Asao-ku, Kawasaki 215-0004, Japan; E-Mail: tk.sano@ajiko.co.jp

⁶ Forest-Wildlife Research and Development Institute, Forestry Administration, Khan Sen Sok, Phnom Penh 12157, Cambodia; E-Mails: sokhengpiny@yahoo.com (S.H.); vuthydalin@yahoo.com (M.V.)

* Author to whom correspondence should be addressed; E-Mail: dulvrq.3317nau@gmail.com; Tel.: +81-92-642-2868.

External Editors: Nophea Sasaki, H. Ricardo Grau and Andrew Millington

Received: 29 August 2014; in revised form: 28 October 2014 / Accepted: 3 November 2014 /

Published: 14 November 2014

Abstract: The objectives of this study are to: (1) evaluate accuracy of tree height measurements of manual stereo viewing on a computer display using digital aerial photographs compared with airborne LiDAR height measurements; and (2) develop an empirical model to estimate stand-level aboveground biomass with variables derived from manual stereo viewing on the computer display in a Cambodian tropical seasonal forest. We evaluate observation error of tree height measured from the manual stereo

viewing, based on field measurements. RMSEs of tree height measurement with manual stereo viewing and LiDAR were 1.96 m and 1.72 m, respectively. Then, stand-level aboveground biomass is regressed against tree height indices derived from the manual stereo viewing. We determined the best model to estimate aboveground biomass in terms of the Akaike's information criterion. This was a model of mean tree height of the tallest five trees in each plot ($R^2 = 0.78$; RMSE = 58.18 Mg/ha). In conclusion, manual stereo viewing on the computer display can measure tree height accurately and is useful to estimate aboveground stand biomass.

Keywords: aerial photograph; REDD+; stereo viewing; tropical forest; Cambodia

1. Introduction

Reducing emissions from deforestation and forest degradation in developing countries, especially in tropical regions, is recognized as a way to mitigate climate change. For example, the Intergovernmental Panel on Climate Change (IPCC) Fourth Assessment Report states that deforestation in the forest sector is the major factor in total carbon emissions, and tropical forest has the greatest mitigation potential in such sector [1]. An appropriate framework to reduce deforestation and forest degradation is needed [2]. Reducing emissions from deforestation and forest degradation, and the role of conservation, sustainable management of forests and enhancement of forest carbon stocks in developing countries (REDD+), is one example of a framework for climate change mitigation. REDD+ is expected to establish incentives for developing countries to protect and better manage their forest resources, by creating and recognizing financial value for the additional carbon stored in trees or not emitted to the atmosphere [3]. REDD+ activities must be based on scientifically robust forest monitoring systems [4].

Currently, remote sensing with ground-based inventories is recommended for forest monitoring systems, because remotely sensed data can be collected easily even for difficult places to access for field surveys, and the data acquired have consistency and transparency [5]. Light detection and ranging (LiDAR) is well suited to tree height, biomass, and other forest structural attribute measurement and estimation (e.g., [6–8]), and is currently the most accurate remote sensing system to obtain specific site-level data on forest structure and aboveground biomass. Although aircraft sensors such as LiDAR cover relatively small areas, forest carbon stocks calculated from airborne LiDAR can be used as values representative of each forest area to estimate those stocks across a country [9]. However, high acquisition cost and data volume hinder repeated monitoring of large forest areas [10]. Therefore, investigations of alternative approaches using remote sensing data are useful for forest monitoring systems. In addition to airborne LiDAR estimation, there are a lot of previous studies, which estimated aboveground biomass with different types of remote sensing data in tropical forests. Optical satellite data has been frequently used to obtain aboveground biomass in forests (e.g., [11–13]). Radar remote sensing has also been used to quantify forest biomass (e.g., [14–18]). However, biomass estimation with SAR in dense tropical forests is still a challenging task although a new approach to estimate and map aboveground biomass in tropical forests is now investigated in the BIOMASS mission [19].

Aerial photographs have been used for many decades in forest inventory [20]. Quantitative and qualitative forest characteristics have been measured by manual methods of stereo photogrammetry (3D methods hereafter) using aerial photographs since the 1940s [21]. Progress in computer science, however, enables production of digital surface models (DSMs) automatically from a stereo pair of digital aerial photographs using stereo matching algorithms similar to those derived from airborne LiDAR first returns. A DSM from high spatial resolution digital aerial photographs can predict tree height, biomass, and other forest structural attributes very accurately, as accurate as airborne LiDAR estimation [22,23]. Progress in computer science also facilitates manual 3D stereo viewing methods on computer displays using digital aerial photographs and shuttered glass (manual stereo viewing hereafter), similar to conventional 3D methods using misreading-prone and a skill-demanding parallax bar on a hardcopy image. Manual stereo viewing is intuitive and there is no need for technical skills for measurement. Thus, investigation of tree height measurement and biomass estimation accuracy of manual stereo viewing may furnish another means for estimating carbon stocks and another option for forest monitoring systems. Nevertheless, there is very little research on this accuracy.

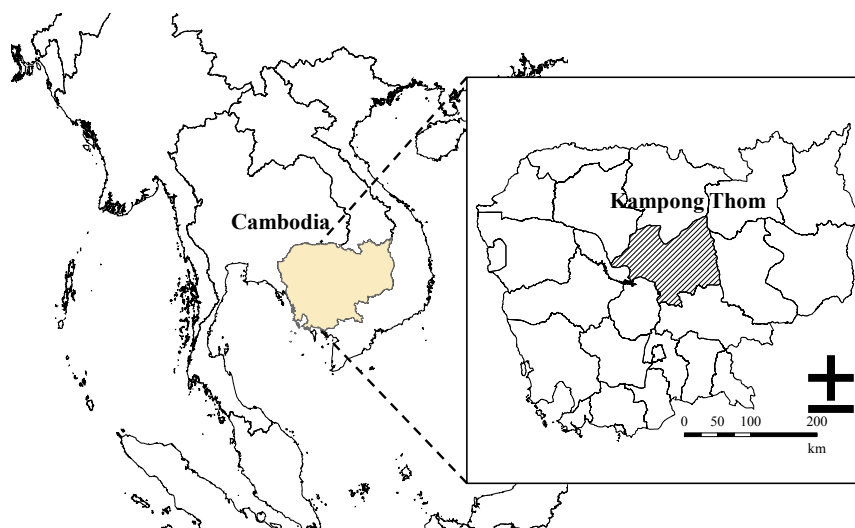
The objectives of our study are to: (1) evaluate accuracy of tree height measurement of manual stereo viewing on a computer display using digital aerial photographs compared with airborne LiDAR height measurement; and (2) develop an empirical model to estimate stand-level aboveground biomass with variables derived from manual stereo viewing for a tropical seasonal forest.

2. Study Area and Remote Sensing Data

2.1. Study Area

The study area is in Kampong Thom Province, central Cambodia (Figure 1). This province is 1,244,764 ha in area. The rainy season is May through October and the dry season November through April, with 1700 mm annual precipitation [24]. Topography is lowland and nearly flat, with elevations from 1 to 80 m above sea level. The study area has three forest types, evergreen, degraded evergreen, and deciduous. Degraded is defined here as an evergreen forest with evidence of illegal logging (e.g., stumps) from field survey.

Figure 1. Study area, Kampong Thom Province, Cambodia.



2.2. Remote Sensing Data

We used aerial photographs and airborne LiDAR data. Data from both were acquired on 18–21 January 2012. No deciduous trees were in leaf-off condition. The measurement platform was equipped with a Global Positioning System (GPS) and an Inertial Measurement Unit (IMU). Altitude and tilt information of each aerial photograph and airborne LiDAR data were acquired. Camera focal length was 51.2499 mm. Image size was 8984×6732 pixels and pixel size was $6.0 \mu\text{m}$ inside the camera. Mean altitude of aerial photographs was 510 m above sea level. Airborne LiDAR data were acquired by an ALTM3100 system (Optech, Toronto, ON, Canada) simultaneous with aerial photography. Pulse frequency was 100 kHz and first return density was 26 points/m². Details of aerial photographs and airborne LiDAR data are described in Table 1. From first and last returns, we constructed a 1-m resolution grid of a digital canopy height model (DCHM). The DCHM was calculated by subtracting a digital terrain model (DTM) from a digital surface model (DSM). Standard practices were followed to create the DTM [25]. The DSM was created from the highest first return value of pulses for each grid cell.

Table 1. Details of aerial photograph and airborne LiDAR data acquisition.

Aerial Photograph Acquisition	
CCD	DALSA Sensor + 60.5 Mp Image Sensor 8984 × 6732 Full Frame CCD Color Image Sensor
Number of pictures	16
Acquisition date	18–21 January 2012
Focal length (mm)	51.2499
Scale (pixels)	8984 × 6732
Pixel size (μm)	6.0
Ground resolution (cm)	7
Acquisition altitude (m)	478–545
Airborne LiDAR Data Acquisition	
LiDAR system	ALTM 3100
Flight altitude (m)	510
Pulse frequency (kHz)	100
Scan frequency (kHz)	53
Flight speed (m/s)	25

3. Methods

First, we conducted field survey. Trees located along a roadside were measured for the evaluation of tree height measurements from manual stereo viewing. Field data were also collected within permanent plots. Aboveground biomass of each permanent plot (Mg/ha) were calculated from field data. Then, we evaluated observation error of tree height measured from the manual stereo viewing based on field measurements. We performed tree height measurements by manual stereo viewing using digital aerial photographs. The measurements were compared with tree height measurements from field survey. Finally, we developed biomass estimation models based on tree height measurements

from manual stereo viewing. Aboveground biomass was regressed against indices calculated from height measurements using by manual stereo viewing using digital aerial photographs

3.1. Field Survey

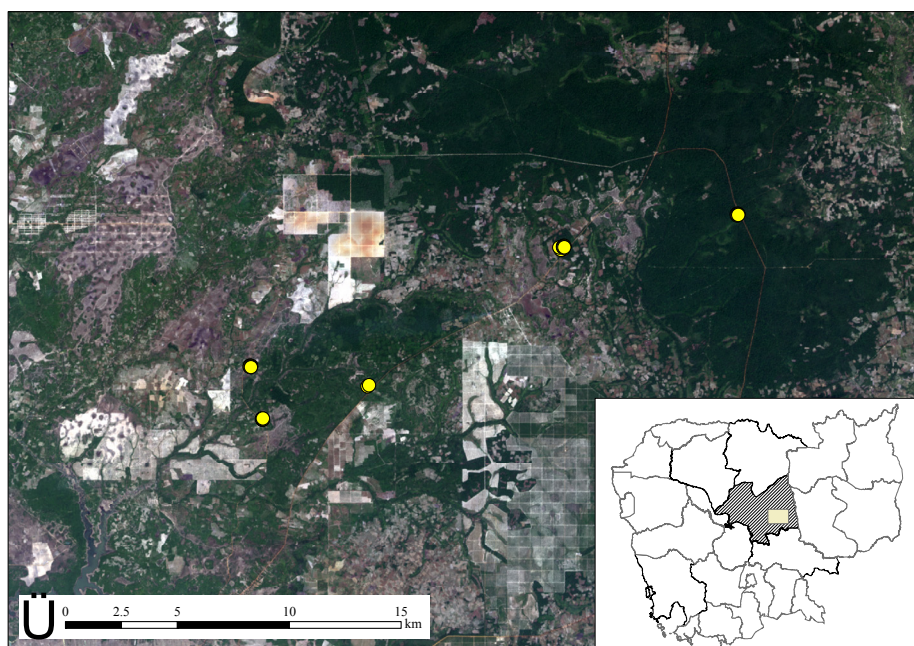
To evaluate tree height measurement accuracy, we selected 17 trees in an evergreen forest and measured the heights during field survey. In that survey, tree height measurement in permanent plots is likely to include relatively large error, because it is often difficult to see treetops in dense forests like evergreen. Therefore, we selected trees located along a roadside and not within permanent plots for evaluating measurement accuracy. We used Vertex III (Haglof Sweden, Långsele, Sweden) for all tree height measurement. Measurements were done twice and we considered the average of these as tree height.

There were 38 permanent plots in the study area, which included 32 plots of 0.09 ha and six of 0.08 ha (Figure 2; 12 in evergreen forest, 11 in degraded evergreen forest, and 15 in deciduous forest). The location of all plots was measured by GPS. Because the GPS instrument we used was not a differential GPS receiver, the accuracy of plot corner coordinates determined by the GPS instrument was open to question. Therefore, we checked these coordinates in the field in May 2013. We selected the most reliable GPS corner coordinated for each plot comparing with a tree position map created from field measurements, aerial photographs, and forest structures in the field. From the selected corner, we determined the other corners mathematically from the size and azimuth direction of each plot. We measured DBH (Diameter at Breast Height), tree height and tree species for all trees that were larger than 5 cm in DBH. Then we calculated the aboveground biomass of each tree using the biomass estimation model developed by Brown [26];

$$Biomass = 42.69 - 12.800DBH + 1.242(DBH)^2 \quad (1)$$

where *Biomass* = aboveground biomass (kg), *DBH* = diameter at breast height (cm).

Figure 2. Location of permanent sample plots.



3.2. Evaluation of Tree Height Measurement Accuracy of Manual Stereo Viewing

Tree height measurement was performed for 17 selected trees by manual stereo viewing, using digital aerial photographs and a DCHM from airborne LiDAR data. Although not all trees were identified, the identified species of measured trees were *Sindora siamensis*, *Diospyros bejaudii*, *Peltophorum dasyrhachis*, *Dipterocarpus alatus*, *Lophopetalum dupperreanum* and *Chionanthus thorelii*. This measurement was done using Stereo Viewer Pro version 2.02 (Photec, Sapporo-shi, Japan). This software requires altitude and tilt information of each aerial photograph to conduct manual stereo viewing for the measurement. Tree height was calculated by subtracting tree base elevation from tree top elevation. For the 17 trees, we defined road elevation as tree base elevation, because the topography was nearly flat and all trees were located along the roadside. First, an interpreter measured road elevation near the trees and detected their tops, then each tree top elevation was measured. The spatial distribution (longitude, latitude, and altitude) of each tree top was automatically registered and tree height was automatically calculated by Stereo Viewer Pro.

Tree height measurement of the DCHM from airborne LiDAR data was done using ArcMap version 10.1 (ESRI, New York, NY, USA). We defined the highest DCHM height of each tree as tree height. We superimposed the treetop data layer from aerial photographs on the DCHM layer to confirm that we had measured the same trees with Stereo Viewer Pro and ArcMap.

We defined as error the difference between tree height measured via manual stereo viewing or DCHM from airborne LiDAR and the field survey height. To evaluate the accuracy of tree height measurement, we compared Root Mean Square Error (RMSE) of manual stereo viewing and that of DCHM from airborne LiDAR data. RMSEs were calculated as follows.

$$RMSE = \sqrt{\frac{1}{n} \sum_{i=1}^n (X_i - x_i)^2} \quad (2)$$

where X_i = tree height measured from field survey of the i th tree; x_i = tree height measured from manual stereo viewing or DCHM from airborne LiDAR data of the i th tree; and n = number of measured trees (*i.e.*, 17).

3.3. Stand-Level Aboveground Biomass Estimation

Stand-level aboveground biomass estimation models were developed with 38 permanent plots. This biomass from field survey were used as response variables. Tree height indices and a tree density index derived from manual stereo viewing were investigated as explanatory variables. Tree height measurement with manual stereo viewing was done for each plot and all visible trees from aerial photographs were measured. Tree height indices and a tree density index were calculated from results of these tree height measurements. We developed two estimation models using two types of explanatory variables; one is based on all measured trees from manual stereo viewing and the other is based on specific parts of them.

Based on all measured trees from manual stereo viewing, we investigated three tree height indices, which were mean tree height, mean overstory height and median tree height of each plot. We defined tree height indices as follows. Mean tree height is that of all trees in each plot. Mean overstory height is mean tree height of the tallest 50% trees in each plot. Median tree height is for each plot. In addition,

we examined whether a combination model of tree height indices and tree density index improved the biomass estimation model. We used tree density per hectare calculated by visible trees from aerial photographs in each plot as a tree density index.

Apart from the estimation model using all measured trees, we tested how many trees we should measure per plot to obtain a certain accuracy for the biomass estimation. We investigated mean tree height of the tallest x trees in each plot as tree height indices (x from 1 to 16). Mean height of all measured trees were used, if the number of measured trees was less than x .

To develop estimation models, we tested candidate estimation models as follows.

$$\log(\text{Biomass}) = \log\alpha + \beta\log H \quad (3)$$

$$\log(\text{Biomass}) = \log\alpha + \beta\log H + \gamma\log N \quad (4)$$

$$\text{Biomass} = \alpha H + \beta \quad (5)$$

$$\text{Biomass} = \alpha H + \beta N + \gamma \quad (6)$$

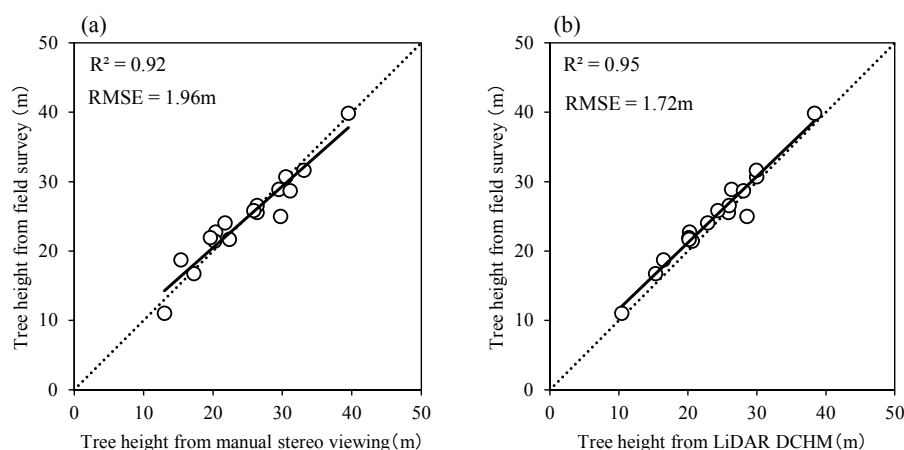
where H is the tree height index (m), N is the tree density index (trees/ha), and α , β and γ are regression coefficients. The best estimation models were determined for each type of explanatory variables in terms of the Akaike's information criterion (AIC). For the aboveground biomass estimation models, RMSE of observed and predicted aboveground biomass were also calculated. All analyses were conducted using R software version 2.15.2.

4. Results

4.1. Tree Height Measurement Accuracy of Manual Stereo Viewing

The results of tree height measurement using manual stereo viewing and DCHM from airborne LiDAR data are shown in Figure 3. In the field survey, tree heights of the 17 trees ranged from 11.1 m to 39.9 m, and mean height was 24.8 m. In the measurement of manual stereo viewing and DCHM from LiDAR, tree heights were from 13.0 m to 39.5 m and 10.4 m to 38.3 m, respectively, and corresponding mean heights were 24.8 m and 23.7 m. RMSEs of manual stereo viewing and of the DCHM from airborne LiDAR data were 1.96 m and 1.72 m, respectively.

Figure 3. Result of tree height measurement in manual stereo viewing and DCHM from LiDAR. (a) Manual stereo viewing; (b) DCHM from LiDAR data.



4.2. Stand-Level Aboveground Biomass Estimation

In the field survey, mean stand-level aboveground biomass of 38 plots was 170.94 Mg/ha, with a range from 8.98 Mg/ha to 481.80 Mg/ha. The number of measured trees per plot ranged from five to 42, and the average was 16.55. Figure 4 shows the tree height distribution of all trees from the measurement of manual stereo viewing and the field survey. Mean tree height of the measurement of manual stereo viewing was 15.7 m and that of the field survey was 10.5 m. Kolmogorov-Smirnov test showed that tree height distribution measured from manual stereo viewing was significantly different from that measured from field survey ($p < 0.05$).

Figure 4. Empirical cumulative distribution function and tree height distribution for all measured trees from the manual stereo viewing and the field survey.

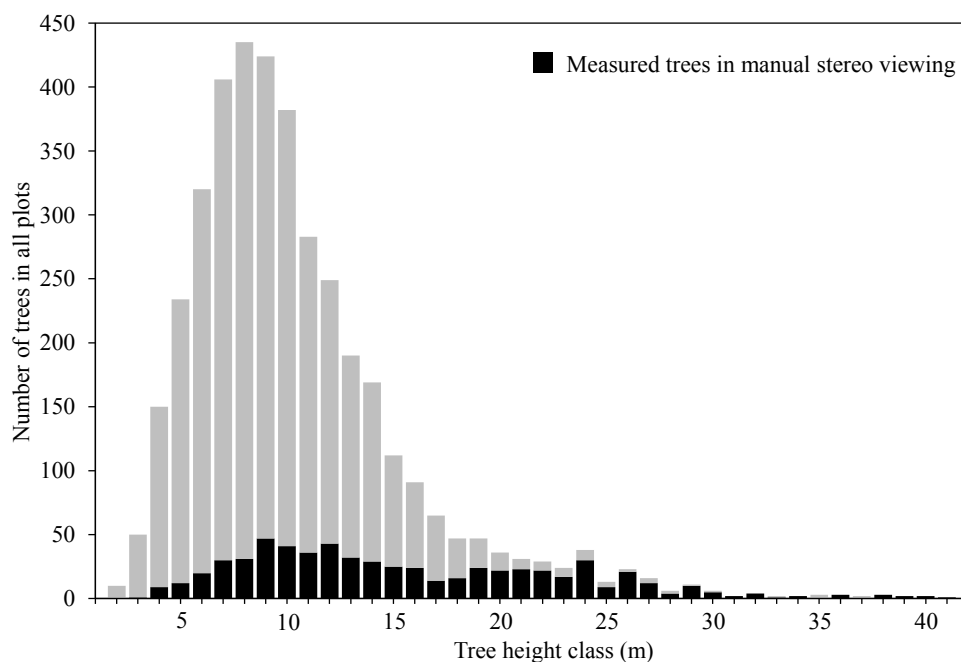


Table 2 shows the result of regression analysis based on all measured trees from manual stereo viewing. This analysis showed that logarithmic mean overstory height (Equation (3)) was the best single explanatory variable for biomass estimation ($AIC = 429.2$ and $R^2 = 0.74$). RMSE of observed and predicted stand-level aboveground biomass was 63.36 Mg/ha (Figure 5a). For combined tree density and tree height indices, logarithmic mean tree height and tree density per hectare (Equation (4)) were selected as the best aboveground biomass estimation model ($AIC = 426.1$ and $R^2 = 0.77$); RMSE was 59.28 Mg/ha (Figure 5b). All combination regression models of tree density index and tree height indices improved RMSE and R^2 compared with those of the single tree height index.

Table 2. Results of regression analysis for biomass estimation model.

	Variables	AIC	R ²	RMSE (Mg/ha)	RMSE (%)	Link
Single	H_{mean}	429.3	0.74	63.45	37.12	identity
	$H_{overstory}$	429.7	0.74	63.78	37.31	identity
	H_{median}	436.3	0.69	69.62	40.73	Identity
	N	480.5	0.00	124.44	72.80	identity
	$\log(H_{mean})$	432.0	0.72	65.77	38.48	log
	$\log(H_{overstory})$	429.2	0.74	63.36	37.07	log
	$\log(H_{median})$	438.3	0.67	71.47	41.81	log
	$\log(N)$	480.5	0.00	124.46	72.81	log
Multiple	H_{mean}, N	428.1	0.76	60.89	35.62	identity
	$H_{overstory}, N$	431.6	0.74	63.77	37.31	identity
	H_{median}, N	435.6	0.71	67.14	39.28	identity
	$\log(H_{mean}), \log(N)$	426.1	0.77	59.28	34.68	log
	$\log(H_{overstory}), \log(N)$	430.6	0.75	62.91	36.80	log
	$\log(H_{median}), \log(N)$	435.3	0.71	66.93	39.15	log

H_{mean} : mean tree height, $H_{overstory}$: mean overstory height, H_{median} : median tree height, N : tree density per hectare.

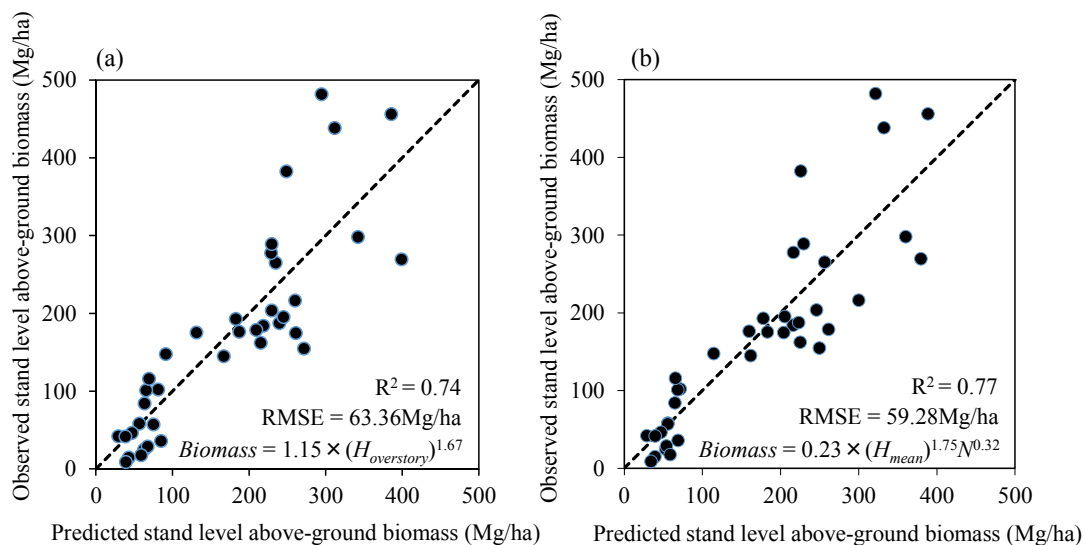
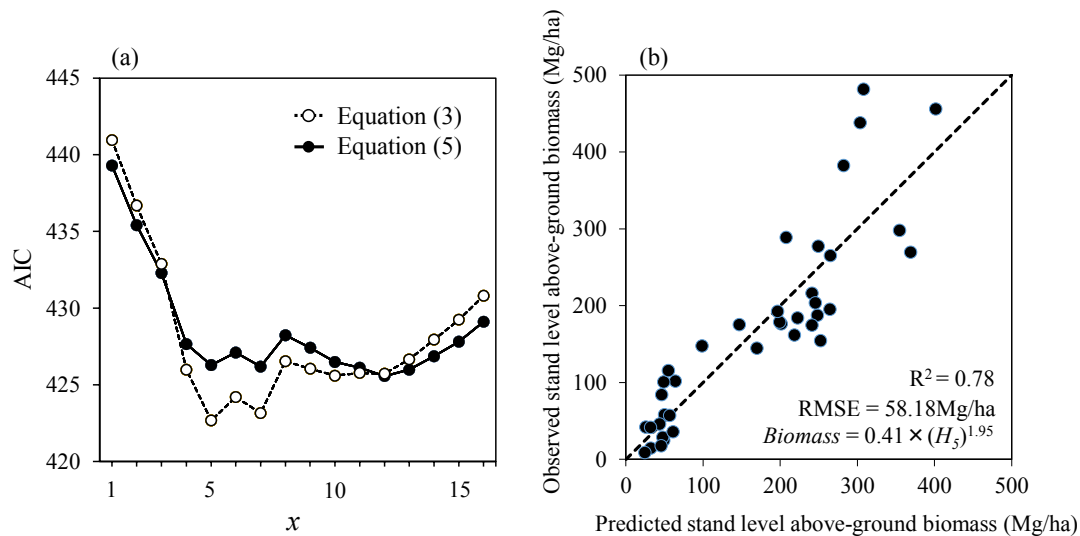
Figure 5. Observed and predicted biomass estimation: (a) one variable; (b) two variables.

Figure 6 shows the result of regression analysis for mean tree height of the tallest x trees in each plot. Mean tree height of the tallest five trees with logarithmic model (Equation (3)) was the best model (AIC = 422.7 and $R^2 = 0.78$). RMSE of observed and predicted stand-level aboveground biomass was 58.18 Mg/ha, corresponding to 34.0%.

Figure 6. Result of regression analysis for mean tree height of the tallest x trees in each plot: (a) AIC (x from one to 16); (b) Observed and predicted biomass estimation for the best model ($x = 5$).



5. Discussion

We investigated the accuracy of tree height measurement and aboveground biomass estimation of manual stereo viewing for a tropical seasonal forest. RMSE of tree height measurement of manual stereo viewing was 1.96 m. Gong *et al.* [27] investigated the accuracy of tree height measurement using digital aerial photographs without shuttered glass (a method of adjusting the same point in each aerial photograph to measure parallax), finding an RMSE of 2.30 m (1.96 m in our study) for 41 redwood trees. Vastaranta *et al.* [22] gave a tree height accuracy of 11.2% for RMSE (7.9% in our study) with a DSM derived from a stereo matching algorithm using digital aerial photographs. Our study is comparable with these works, which used methods without shuttered glass and a stereo matching algorithm in temperate forests.

We found RMSE of DCHM from airborne LiDAR data to be 1.72 m. Accuracy of tree height measurement of manual stereo viewing was nearly the same as measurement of the DCHM from airborne LiDAR data. Measurement of tree height using airborne LiDAR data had high accuracy and reliability [28,29]. Thus, using manual stereo viewing is a feasible way to measure tree height. However, it should be noted that not all trees are detected using manual stereo viewing. Understandably, manual stereo viewing detects only the trees of upper layer in forests because lower trees are hidden by upper trees. In this study, trees, which were less than 20m in height, were difficult to detect using manual stereo viewing (Figure 4). Tree height distribution measured from manual stereo viewing was also significantly different from that measured from field survey. Therefore, mean tree height of the measurement of manual stereo viewing was higher than that of the field survey. Manual stereo viewing was not a real alternative for field measurement.

Regression analysis showed that logarithmic mean overstory height was the best single variable for biomass estimation based on all measured trees from manual stereo viewing (Table 2), and the combination model of logarithmic mean tree height and tree density per hectare was slightly better in terms of RMSE, AIC and R^2 than a single variable aboveground biomass estimation model.

These results show that combination models of tree height indices and tree density index can improve aboveground biomass estimation accuracy, although the tree density index alone cannot be used to estimate that biomass. Regression analysis using the tallest x trees showed that logarithmic model using the tallest five trees per plot was the best within the tallest x trees models and the tallest five trees was better than the best combination model using all measured trees in terms of RMSE, AIC and R^2 . Moreover, the logarithmic model using the tallest five to ten trees were better than regression model using all measured tree. It seems to be preferable because of time saving in practical use. We conclude that the measuring the tallest five to ten trees per plot was enough to obtain a certain accuracy for stand level biomass estimation, although it may be difficult to select the tallest five trees among other candidate trees within plots.

Compared with previous studies using airborne LiDAR, aboveground biomass estimation from manual stereo viewing can be comparable with that of airborne LiDAR data. Mascaro *et al.* [30] reported that the accuracy of aboveground carbon density estimation using these data was $R^2 = 0.84$ and $RMSE = 17 \text{ Mg}\cdot\text{C}/\text{ha}$, corresponding to 17.6% of the mean density in Panama. For biomass estimation in the United States, Lefsky *et al.* [6] reported $R^2 = 0.80$ and $RMSE = 75.1 \text{ Mg}/\text{ha}$, corresponding to 31.8%. These studies suggest that the accuracy of aboveground biomass estimation using tree height from manual stereo viewing in our study ($R^2 = 0.78$ and $RMSE = 58.18 \text{ Mg}/\text{ha}$, corresponding to 34.0%) is comparable with that of airborne LiDAR estimation, especially in terms of R^2 .

Being comparable with aboveground biomass estimation using airborne LiDAR, manual stereo viewing can be used for aboveground biomass estimation in forest management. Brown *et al.* [31] showed that an aerial photograph with ground-based inventory approach was three times more cost effective than conventional field methods. In addition, measurement data of manual stereo viewing are recorded in digital format, in contrast to conventional 3D methods on hard copy images. This leads to robust transparency of biomass estimation in REDD+ forest monitoring systems, because measurement results can be confirmed by a third party. Operationally, manual stereo viewing can be used as references for REDD+. Asner *et al.* [32] demonstrated that biomass estimated from airborne LiDAR and field measurement was available as reference data for large area biomass estimation. The estimated biomass using manual stereo viewing may be available as the alternative of airborne LiDAR data, which is used by Asner *et al.* [32]. In conclusion, manual stereo viewing is a method of moderate accuracy in biomass estimation, with cost effectiveness and robust transparency, and is useful for forest monitoring systems in tropical regions.

However, there are limitations in this biomass estimation approach. We assumed no variation in wood specific gravity for biomass estimation models although it is an important predictor for biomass estimation [33]. This could lead estimation errors when wood specific gravity varies according to environmental change. In addition, this method is still needed to be investigated for REDD+ forest monitoring systems. Further studies to improve the accuracy and utility of this method should be pursued. Tree height measurement of manual stereo viewing requires roads near forests or gaps in forests as a substitute for tree base elevation. Studies are required to assess the utility of this method for the forests, in which there are neither gaps nor roads. Also, studies in steep forests are required to validate the utility of the method for various kinds of topography.

6. Conclusions

We investigated accuracy of tree height measurement and stand-level aboveground biomass estimation of manual stereo viewing on a computer display using digital aerial photographs in a Cambodian tropical seasonal forest. Accuracy of tree height measurement of manual stereo viewing was nearly the same as measurement of the DCHM from airborne LiDAR data. Also, the model using variables derived from manual stereo viewing was comparable with previous studies that used LiDAR data to estimate biomass and aboveground carbon density. In conclusion, manual stereo viewing on the computer display can measure tree height accurately and is useful to estimate aboveground stand biomass.

Acknowledgments

This study is part of the project “Technology Development for Circulatory Food Production Systems Responsive to Climate Change”, supported by the Ministry of Agriculture, Forestry and Fisheries, Japan.

Author Contributions

Katsuto Shimizu analyzed most of the data in this study and wrote the entire manuscript. Tetsuji Ota and Tsuyoshi Kajisa reviewed the manuscript and gave suggestions about analyses and conceptualization. Nobuya Mizoue and Shigejiro Yoshida supervised and made suggestions. They also reviewed and commented on the manuscript, as did Gen Takao, Yasumasa Hirata, and Naoyuki Furuya. Takio Sano contributed to acquiring aerial photographs and airborne LiDAR data of Cambodia. Sokh Heng and Ma Vuthy obtained permission to perform research in Cambodia and contributed their significant knowledge of Cambodian forests.

Conflicts of Interest

The authors declare no conflict of interest.

References

1. Nabuurs, G.J.; Masera, O.; Andrasko, K.; Benitez-Ponce, P.; Boer, R.; Dutschke, M.; Elsiddig, E.; Ford-Robertson, J.; Frumhoff, P.; Karjalainen, T.; *et al.* Forestry. In *Climate Change 2007: Mitigation. Contribution of Working Group III to the Fourth Assessment Report of the Intergovernmental Panel on Climate Change*; Metz, B., Davidson, O.R., Bosch, P.R., Dave, R., Meyer, L.A., Eds.; Cambridge University Press: Cambridge, UK, 2007; pp. 541–584.
2. Hall, A. Better RED than dead: Paying the people for environmental services in Amazonia. *Philos. Trans. R. Soc. B* **2008**, *363*, 1925–1932.
3. Corbera, E.; Schroeder, H. Governing and implementing REDD+. *Environ. Sci. Policy* **2011**, *14*, 89–99.

4. Böttcher, H.; Eisbrenner, K.; Fritz, S.; Kindermann, G.; Kraxner, F.; McCallum, I.; Obersteiner, M. An assessment of monitoring requirements and costs of “Reduced emissions from deforestation and degradation”. *Carbon Balance Manag.* **2009**, *4*, doi:10.1186/1750-0680-4-7.
5. Kiyono, Y. Measurement, reporting and verification (MRV) of forest monitoring. In *REDD-Plus Cookbook How to Measure and Monitor Forest Carbon*; FFPRI: Tsukuba, Japan, 2012; pp. 22–25.
6. Lefsky, M.A.; Harding, D.; Cohen, W.B.; Parker, G.; Shugart, H.H. Surface LiDAR remote sensing of basal area and biomass in deciduous forests of eastern Maryland, USA. *Remote Sens. Environ.* **1999**, *67*, 83–98.
7. Drake, J.B.; Dubayah, R.O.; Knox, R.G.; Clark, D.B.; Blair, J.B. Sensitivity of large-footprint Lidar to canopy structure and biomass in a neotropical rainforest. *Remote Sens. Environ.* **2002**, *81*, 378–392.
8. Ioki, M.; Imanishi, J.; Sasaki, T.; Morimoto, Y.; Kitada, K. Estimating stand volume in broad-leaved forest using discrete-return LiDAR: Plot-based approach. *Landsc. Ecol. Eng.* **2010**, *6*, 29–36.
9. Gibbs, H.K.; Brown, S.; Niles, J.O.; Foley, J.A. Monitoring and estimating tropical forest carbon stocks: Making REDD a reality. *Environ. Res. Lett.* **2007**, *2*, doi:10.1088/1748-9326/2/4/045023.
10. Pflugmacher, D.; Cohen, W.B.; Kennedy, R.E.; Yang, Z. Using Landsat-derived disturbance and recovery history and Lidar to map forest biomass dynamics. *Remote Sens. Environ.* **2014**, *151*, 124–137.
11. Steininger, M.K. Satellite estimation of tropical secondary forest above-ground biomass: Data from Brazil and Bolivia. *Int. J. Remote Sens.* **2000**, *21*, 1139–1157.
12. Kajisa, T.; Murakami, T.; Mizoue, N.; Yoshida, S. Object-based forest biomass estimation using Landsat ETM+ in Kampong Thom Province, Cambodia. *J. For. Res. Jpn.* **2009**, *14*, 203–211.
13. Palace, M.; Keller, M.; Asner, G.P.; Hagen, S.; Braswell, B. Amazon forest structure from IKONOS satellite data and the automated characterization of forest canopy properties. *Biotropica* **2008**, *40*, 141–150.
14. Imhoff, M.L. Radar backscatter and biomass saturation: ramifications for global biomass inventory. *IEEE Trans. Geosci. Remote Sens.* **1995**, *33*, 511–518.
15. Luckman, A.; Baker, J.; Honzák, M.; Lucas, R. Tropical forest biomass density estimation using JERS-1 SAR: Seasonal variation, confidence limits, and application to image mosaics. *Remote Sens. Environ.* **1998**, *63*, 126–139.
16. Santos, J.R.; Freitas, C.C.; Araujo, L.S.; Dutra, L.V.; Mura, J.C.; Gama, F.F.; Soler, L.S.; Sant’Anne, S.J.S. Airborne P-band SAR applied to the aboveground biomass studies in the Brazilian tropical rainforest. *Remote Sens. Environ.* **2003**, *87*, 482–493.
17. Ho Tong Minh, D.; Tebaldini, S.; Rocca, F.; le Toan, T.; Villard, L.; Dubois-Fernandez, P.C. Capabilities of biomass tomography for investigating tropical forests. *IEEE Trans. Geosci. Remote Sens.* **2015**, *53*, 965–975.
18. Saatchi, S.; Marlier, M.; Chazdon, R.L.; Clark, D.B.; Russell, A.E. Impact of spatial variability of tropical forest structure on radar estimation of aboveground biomass. *Remote Sens. Environ.* **2011**, *115*, 2836–2849.

19. Ho Tong Minh, D.; le Toan, T.; Rocca, F.; Tebaldini, S.; D'Alessandro, M.M.; Villard, L. Relating P-band synthetic aperture radar tomography to tropical forest biomass. *IEEE Trans. Geosci. Remote Sens.* **2014**, *52*, 967–979.
20. Caylor, J. Aerial photography in the next decade. *J. For.* **2000**, *98*, 17–19.
21. Korpela, I. Individual tree measurements by means of digital aerial photogrammetry. *Silva Fenn. Monogr.* **2006**, *3*, 1–93.
22. Vastaranta, M.; Wolfer, M.A.; White, J.C.; Pekkarinen, A.; Tuominen, S.; Ginzler, C.; Kankare, V.; Holopainen, M.; Hyypä, J.; Hyypä, H.; *et al.* Airborne laser scanning and digital stereo imagery measures of forest structure: Comparative results and implications to forest mapping and inventory update. *Can. J. Remote Sens.* **2013**, *39*, 382–395.
23. Véga, C.; St-Onge, B. Height growth reconstruction of a boreal forest canopy over a period of 58 years using a combination of photogrammetric and LiDAR models. *Remote Sens. Environ.* **2008**, *112*, 1784–1794.
24. Forestry Administration in Cambodia/statistics/Forest Cover and Forestland Categories. Available online: <http://www.forestry.gov.kh/Statistic/Forestcover.htm> (accessed on 10 July 2014).
25. Axelsson, P. Processing of laser scanner data—Algorithms and applications. *ISPRS J. Photogramm.* **1999**, *54*, 138–147.
26. Brown, S. *Estimating Biomass and Biomass Change in Tropical Forests: A Primer*; Food and Agriculture Organization: Rome, Italy, 1997.
27. Gong, P.; Sheng, Y.; Biging, G.S. 3D model-based tree measurement from high-resolution aerial imagery. *Photogramm. Eng. Remote Sens.* **2002**, *68*, 1203–1212.
28. Suárez, J.C.; Ontiveros, C.; Smith, S.; Snape, S. Use of airborne LiDAR and aerial photography in the estimation of individual tree heights in forestry. *Comput. Geosci.* **2005**, *31*, 253–262.
29. Popescu, S.C.; Wynne, R.H.; Nelson, R.F. Estimating plot-level tree heights with LiDAR: Local filtering with a canopy-height based variable window size. *Comput. Electron. Agric.* **2003**, *37*, 71–95.
30. Mascaro, J.; Asner, G.P.; Muller-Landau, H.C.; Breugel, M.; Hall, J.; Dahlin, K. Controls over aboveground forest carbon density on Barro Colorado Island, Panama. *Biogeoscience*. **2011**, *8*, 1615–1629.
31. Brown, S.; Pearson, T.; Slaymaker, D.; Ambagis, S.; Moore, N.; Novelo, D.; Sabid, W. Creating a virtual tropical forest from three-dimensional aerial imagery to estimate carbon stocks. *Ecol. Appl.* **2005**, *15*, 1083–1095.
32. Asner, G.P.; Powell, G.V.N.; Mascaro, J.; Knapp, D.E.; Clark, J.K.; Jacobson, J.; Kennedy-Bowdoin, T.; Balaji, A.; Paez-Acosta, G.; Victoria, E.; *et al.* High-resolution forest carbon stocks and emissions in the Amazon. *Proc. Natl. Acad. Sci. USA* **2010**, *107*, 16738–16742.
33. Chave, J.; Réjou-Méchain, M.; Búrquez, A.; Chidumayo, E.; Colgan, M.S.; Delitti, W.B.; Duque, A.; Eid, T.; Fearnside, P.M.; Goodman, R.C.; *et al.* Improved allometric models to estimate the aboveground biomass of tropical trees. *Glob Change Biol.* **2014**, in press.